C. R. Physique 14 (2013) 192–198

Contents lists available at SciVerse ScienceDirect

Comptes Rendus Physique

www.sciencedirect.com

Crystal growth / Croissance cristalline

Small-volume nucleation

Vers le confinement spatial de la nucléation

Zoubida Hammadi, Nadine Candoni, Romain Grossier, Manuel Ildefonso, Roger Morin, Stéphane Veesler *

CINaM-CNRS, Aix-Marseille Université, Campus de Luminy, 13288 Marseille, France

ARTICLE INFO

Article history:
Available online 16 February 2013

Keywords:
Nucleation
Germination
Growth from solutions
Droplets
Microfluidic

Mots-clés :
Nucléation
Germination
Croissance en solution
Gouttes
Microfluidique

ABSTRACT

The nucleation mechanisms behind crystallized products remain mysterious. In this communication, we describe experiments performed using small volumes, microdroplets, to control nucleation and thus product properties. The effect of small-volume systems on nucleation is discussed.

RÉSUMÉ

Il apparait clairement que l'étape de nucléation est décisive dans le contrôle des propriétés des matériaux. On s'intéresse à son contrôle en suivant deux objectifs : le premier, très fondamental, concerne la détection du germe critique, la théorie de la nucléation et la compréhension des mécanismes ; le second, plus applicatif, concerne la maitrise de la cristallisation des matériaux et de leurs propriétés (pour l'industrie pharmaceutique, la biocristallographie ou la biominéralisation…). C'est dans ce cadre que nous avons mené des expérimentations vers le confinement, la localisation spatiale et temporelle de la nucléation, démontrant les possibilités d'un unique événement de cristallisation.
Dans ce contexte, nous avons développé une approche en deux temps, basée sur la génération de gouttes de petit volume, du nanolitre au femtolitre, en utilisant deux montages différents, mais complémentaires. Un premier outil microfluidique simple et polyvalent a été mis en place pour étudier la nucléation, en réduisant le volume de nucléation au nanolitre. Sans pour autant traiter le problème du confinement, il permet d'accéder à la cinétique de nucléation. L'influence directe du volume de manipulation sur la cristallisation est traitée, dans un second temps, à travers un deuxième outil expérimental que nous avons aussi développé ; utilisant un micro-injecteur couplé à des nano-déplaceurs, il permet d'atteindre des volumes du picolitre au femtolitre et montre la possibilité d'agir sur la nucléation par le confinement.

1. Introduction

It is now well established that the nucleation step is decisive in the control of the properties of crystallized products (pharmaceuticals, biominerals, nanomaterials). However, there is still no comprehensive theory of crystal nucleation from

* Corresponding author.
E-mail address: veesler@cinam.univ-mrs.fr (S. Veesler).

1631-0705/$ – see front matter
http://dx.doi.org/10.1016/j.crhy.2012.12.004

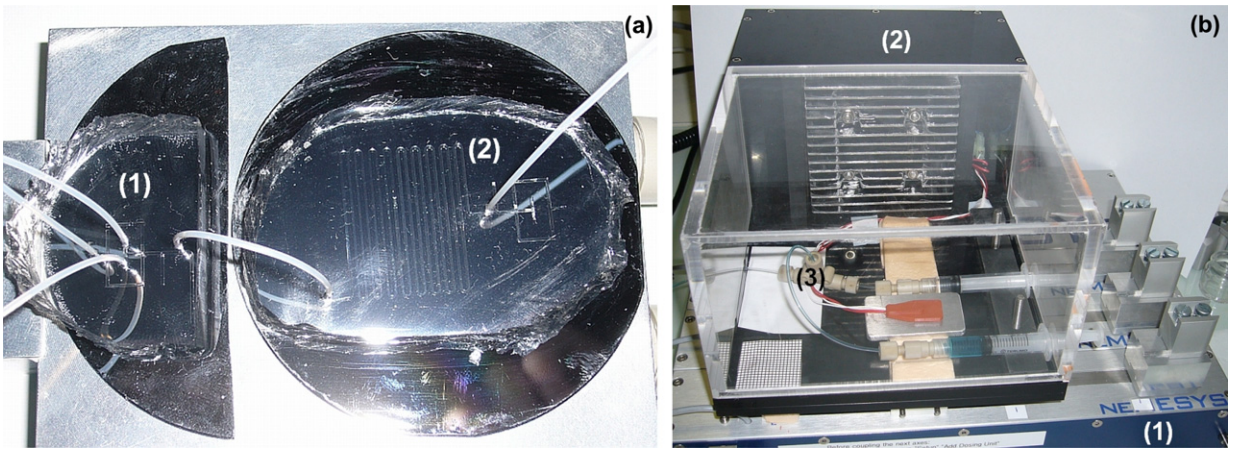

Fig. 1. (a) PDMS microfluidic device, (1) plug-factory and (2) droplet-storage zone, and (b) PEEK/Teflon microfluidic device, (1) syringe pumps, (2) temperature controller (room T to 60 °C) and (3) T-junction.

solution, mainly due to the fact that nucleation is of a stochastic nature: we do not know where and when an indefinite number of nucleation events will occur.

In this communication, we describe experiments we have performed using small volumes, microdroplets, to control nucleation. Microdroplets make observation at the micrometer scale, thus increasing the resolution of detection with an optical microscope, for instance. Microdroplets are also relevant in nucleation studies because they allow a large sample of independent experiments: for instance, 100 identical experiments in 10 nL will yield enough data for statistical analysis of the phenomenon, as compared to 1 experiment in 1 µL. Moreover, a study will require less solute. Our objective being to prove the relevance of small volumes for nucleation studies, we conducted experiments with biological, organic and mineral molecules, all of which follow the same rules [1] concerning crystallization even though each material exhibits specific characteristics.

Two important questions will be addressed here: how can microdroplets be generated and how does volume influence nucleation? We first present a microfluidic approach to generating droplets in order to measure nucleation frequency. Second, via an original approach using confined systems, i.e. small-volume systems whose volume affects nucleation [2], we show a spatial and temporal control of nucleation.

2. Materials

2.1. Generation of microdroplets – Set-ups

2.1.1. Microfluidic devices

We used microfluidic devices in poly(dimethylsiloxane) (PDMS) and polyether ether ketone (PEEK)/Teflon (Figs. 1(a)–1(b)) designed in 2 parts: a plug-factory zone for the mixing and generation of droplets, without surfactant, made of PDMS or composed of a T-junction in PEEK (IDEX P-727 PEEK Tee) and a droplet-storage zone made of PDMS or composed of Teflon tubing (SCI, BB311-24) for the storage and observation of droplets. Droplets were generated at the intersection between the flow of the continuous phase and the liquid of interest. Precision syringe pumps (Bioseb BS-8000 or Nemesys NEM-B101-02) were used to control the flow rates (100–600 µL/h) of droplets and continuous phase. The channel size of the plug-factory, here 500 µm and 584 µm for PDMS and Teflon respectively, determines droplet size (250 nL). Using this set-up, we generated droplets (∼150) of identical volume at a given concentration and we filled storage chips that were stored at different temperatures. During generation and storage, the devices and the feeding syringes were thermostatted. Droplets were observed under a stereomicroscope (Wild Makroskop) equipped with a CCD camera (imaging source, DFK 31BF03).

2.1.2. Nanofluidics for volume confinement

We used a simply-constructed and easy-to-use fluidic device that generates arrayed aqueous phase microdroplets in oil [3] (Figs. 2(a)–2(b)). Up to thousands of microdroplets are generated, with volumes ranging from nanoliter to femtoliter, without surfactant. The device enables the entire volume range to be attained in the course of one experiment. All experiments are performed on an 18 mm diameter hydrophobic coverslip, which can be thermostatted, under an optical microscope. The coverslip is covered with approximately 100 µL of oil. The micrometer-sized droplets of water solution are generated on the coverslip by a microinjector (Femtojet Eppendorf) with a micropipette of 0.5 µm internal diameter (Femtotip Eppendorf). Two home-made micromanipulators (MS30 Mechonics) consisting of 3 miniature translation stages allow displacement of the injector (capillary holder) and the tip in X, Y and Z. Here, we made the sharp tips from tungsten (W) wires (125 µm diameter); for a detailed description see [4–6].

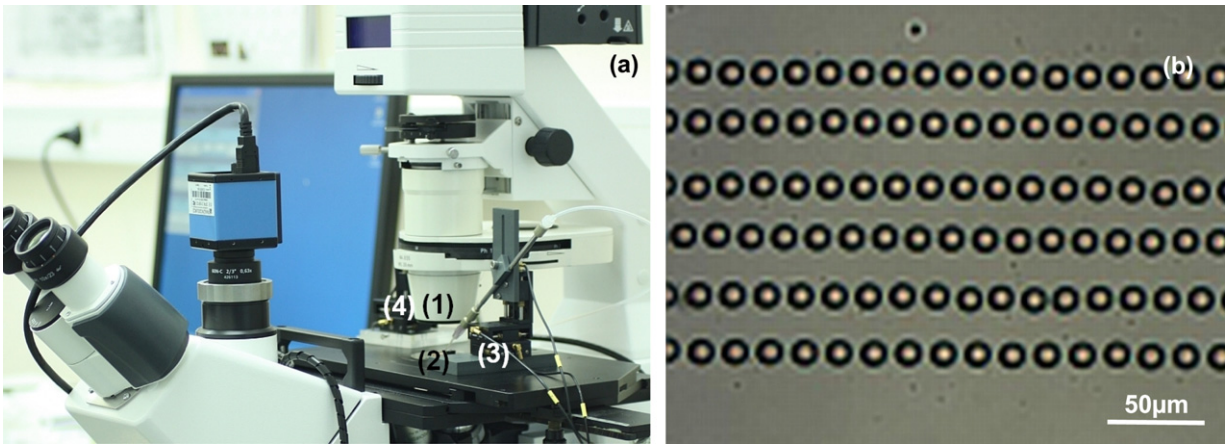

Fig. 2. (a) Image of the whole experimental nanofluidic set-up, (1) microscope, (2) glass micropipette, (3) XYZ miniature translation stages for injector and (4) sharp tungsten tip, and (b) array of monodisperse water droplets (11.8 µm or 0.7 pL).

2.1.3. Multiwell for milliliter crystallization

The apparatus used here is home-made [7] (since marketed by ANACRISMAT). 3 types of vials can be used; here, we used standard HPLC glass vials with 1 mL and 250 µL of solvent. The vials are inserted into two blocks (for 1 mL and 250 µL vials, each block contains 12 and 24 vials respectively) thermostatted independently by Peltier elements and observed under microscope (Nikon Eclipse TE2000-U). The whole assembly is mounted on an X–Y translation table with a Z-control to focus. Sequential image acquisitions are performed automatically and periodically.

2.2. Solutes

2.2.1. Protein solutions

Hen-egg white lysozyme (14 600 Da, pI = 11.2) was purchased from Sigma (batch 057K7013 L 2879) and used without further purification. BPTI (6511 Da, pI = 10.5), was supplied as a lyophilized powder by Bayer and used as received. The purity of both proteins was checked by molecular sieving. Proper amounts of BPTI or lysozyme and NaCl were dissolved in pure water (ELGA UHQ reverse osmosis system) to obtain stock solutions needed for crystallization experiments. The different solutions were buffered with 80 mM acetic acid, adjusted to pH = 4.5 with NaOH (1 M) and filtered through 0.22 µm Millipore filters. The pH was checked with a pH meter (Schott Instruments, ProLab 1000) equipped with a pH microelectrode. Lysozyme and BPTI concentrations were checked by optical density measurements (Biochrom, Libra S22) using an extinction coefficient of 2.64 $\mathrm{mL\,cm^{-1}\,mg^{-1}}$ and 0.786 $\mathrm{mL\,cm^{-1}\,mg^{-1}}$ [8] at 280 nm for lysozyme and BPTI, respectively.

2.2.2. Organic solutions

Caffeine was purchased from Sigma (batch A0283756) and used without further purification. Isonicotinamide was purchased from Sigma (batch BCBD6627) and used without further purification. A suitable amount of caffeine and isonicotinamide was dissolved in ethanol 99% (batch V0D770190D) to obtain the stock solutions required.

2.2.3. Oils

Dodecanemethylpentasiloxane (DMS) oil (Hampton Research HR2-593, refractive index = 1.390 at 20 °C) and Fluorinert™ FC-70 oil (Hampton Research HR2-797, refractive index = 1.303 at 20 °C) were used as continuous phases.

2.2.4. Mineral solutions

KNO_3 (R.P. Normapur, analytical reagent) solutions were prepared by dissolution of the proper amount of powder in pure water.

3. Results and discussion

3.1. Microfluidic crystallization

High-throughput approach, i.e. “automation, miniaturization and parallelization of tasks” [9], was developed in order to rapidly identify crystallization conditions by increasing the number of experiments that can be performed in a given time, while decreasing the quantity of solute used. Microfluidic methods have already proved compatible with this approach, generating droplets of controlled size [10,11], and is also valuable for the control and the study of crystallization processes [12–17]. We recently developed a universally solvent-compatible microfluidic device for crystallization studies [18]. Theoretically, this PEEK/Teflon microfluidic device, adapted from a PDMS device developed by Laval et al. [11], is ideal for studying

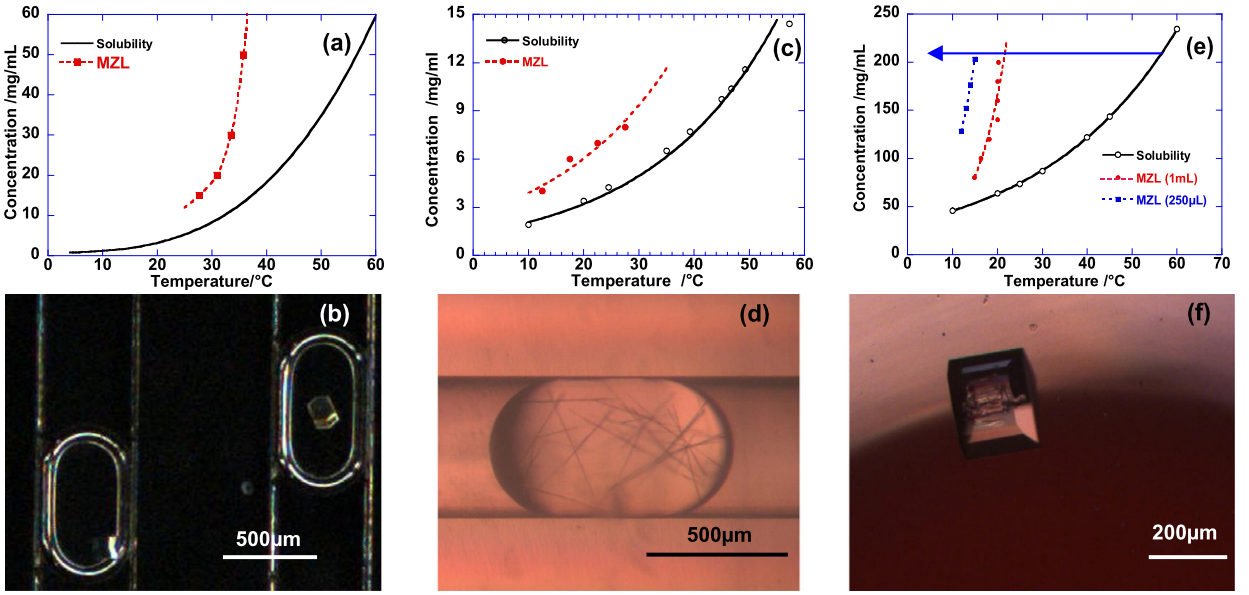

Fig. 3. Solubility and MZ limit, (a) lysozyme in NaCl 0.7 M and pH = 4.5 (device in PDMS), (c) caffeine in ethanol (device in PEEK/Teflon) after [18] with permission of ACS and (e) isonicotinamide in ethanol (multiwell of 1 mL and 250 µL). (b) Lysozyme crystals in aqueous droplets, (d) caffeine crystals in ethanol droplet and (f) crystal of isonicotinamide in ethanol. For experimental procedures see Refs. [7,18,21].

crystallization. It makes it possible to study crystallization of all solutes whatever the medium of crystallization: aqueous or organic solvents.

This communication describes one application of the device: the determination of the metastable zone limit (MZ limit). The metastable zone represents a kinetic limit in the supersaturated region of the phase diagram below which no nucleation occurs for a given time in a given volume. It is thus of interest in the control of the crystallization process. Figs. 3(a)–3(d) show the MZ limit and crystals of lysozyme in aqueous solution and caffeine in ethanol determined using microfluidic devices. In these experiments, supersaturation is achieved by decrease of temperature.

We also focus on nucleation frequency, which depends on volume: the smaller the volume, the longer the induction time, thus requiring greater supersaturation for nucleation, namely a kinetic effect. Small volumes thus increase the supersaturation range experimentally accessible [19]. However, they can be a limitation for a given solute-solvent, depending on the way supersaturation is achieved. As a result, here we were unable to detect any significant nucleation in 250 nL microfluidic crystallizers for isonicotinamide in ethanol, in the supersaturation range accessible with our set-up. Supersaturation is generated by first dissolving the solute at high temperature and then once the desired quantity is dissolved, decreasing temperature, as indicated by an arrow in Fig. 3(e). The highest temperature attainable with our set-up is 60 °C, thus the maximum concentration inside the syringe is 200 mg/mL (for larger concentrations there is a risk of unwanted nucleation inside the syringe before droplet generation). To confirm that induction time is inversely proportional to nucleation volume, we perform experiments on larger volumes, 1 mL and 250 µL, using a multiwell set-up. Results are shown in Figs. 3(e) and 3(f): a decrease of 6.5 °C in the MZ limit is observed when the volume decreases from 1 mL to 250 µL (volume divided by 4). Consequently, for a volume of 250 nL (volume divided by 10^3), the MZ limit is in the negative range of temperature, explaining the absence of nucleation of isonicotinamide in ethanol in our microfluidic device.

To overcome this problem, we propose two solutions: (1) changing the way supersaturation is achieved; or (2) using an external field. In the microfluidic device used in this study, temperature is usually used to achieve supersaturation, but another simple solution can easily be implemented: mixing different solutions, for instance a protein with an agent of crystallization or a solvent acting as an antisolvent, in order to rapidly reach the supersaturated stage. A T-junction can be added before the plug-factory zone to mix solutions. For instance, highly-supersaturated lysozyme solutions are generated by mixing a NaCl solution with a lysozyme solution in a buffer.

External fields to launch nucleation were previously tested successfully in batch crystallizers in the milliliter range [20]. An application of this approach in small volumes is presented in Section 3.2.

3.2. Influence of volume on nucleation

3.2.1. Theoretical considerations

The classical nucleation theory (CNT) supposes an infinite reservoir of molecules, in other words concentration and supersaturation remain constant during the nucleation event. When volume is decreased, the total number of molecules of the system is decreased and the reservoir of molecules becomes finite, in contradiction to the CNT.

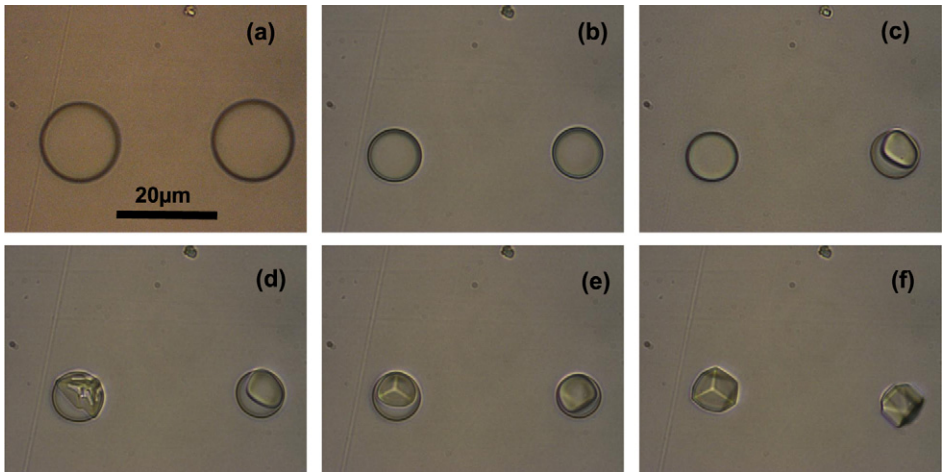

Fig. 4. Nucleation and growth of KNO_3 (1.9 M) in H_2O in FC-70 oil, (a) droplet size 15 µm (2 pL) at $t = 0$, (b) droplet size 9.3 µm (0.48 pL), $t = 8$ min 29 s, (c) $t = 9$ min 15 s, (d) $t = 9$ min 17 s, (e) $t = 10$ min 18 s and (f) $t = 12$ min 12 s.

A simple way to illustrate this influence is to express the supersaturation as it is really experienced during the nucleation process, which consists of the addition of molecules to the forming cluster:

$$\beta(n) = \beta_0 - \frac{n}{N_s} \tag{1}$$

with N_s the number of molecules a droplet has at saturation (size of the system), n the number of molecules in the forming cluster, β_0 and $\beta(n)$ initial and current supersaturations. Replacing n by n^*, the number of molecules in the critical nucleus, we obtain the supersaturation, $\beta(n^*)$, at the moment of formation of the critical nucleus, that is to say at the moment of the nucleation of the first crystal.

In infinite volume, when $N_s \to \infty$; $\beta(n^*) = \beta_0$, thus the CNT is verified.

When volume is decreased, N_s becomes finite and $\beta(n^*) < \beta_0$, thus increasing the critical size and the energy barrier that need to be reached. In other words, the smaller the crystallization volume the more difficult the nucleation. As a result, in these small-volume systems unexpected high-supersaturated metastable solutions are observed. In practice, there is an influence of volume on nucleation from picoliter range down [2]. This is in agreement with experimental results showing effects under nanoscopic confinement [22–26].

To summarize, nucleation experiments conducted with microfluidic set-ups in the nanoliter range are in agreement with the CNT, meaning that they are representative of nucleation in infinite volume, apart from a kinetic effect (the smaller the volume, the longer the induction time). Whereas nucleation experiments conducted with our nanofluidic set-up in the nanoliter to femtoliters range are subject to an added thermodynamic effect that stabilizes high-supersaturated solutions.

3.2.2. Practical applications

We conducted two sets of nucleation experiments in small volumes, one by evaporation and the other launched by a mechanical contact using a tip.

In the first, after generating droplets of 1.9 M KNO_3 in water, we monitored the diffusion of water into the oil leading to increasing KNO_3 concentration until nucleation (Figs. 4(a)–4(d)) and both nucleation events are single. Interestingly, single crystals nucleated were rough and a transition from growth form to equilibrium form was observed in less than 3 minutes (Figs. 4(c)–4(f)). The supersaturation at the moment of nucleation is high and can be conservatively estimated from the decrease in droplet volumes between Figs. 4(a) and 4(b), making the simple assumption that concentration remains constant between Figs. 4(b) and 4(c). Droplet diameter decreases from 15 to 9.3 µm, thus volume decreases by a factor of 0.238. The concentration is thus $1.9/0.238 = 7.98$ M, a value larger than that obtained (7.07 M) by Laval et al. [27] in their experiments on KNO_3 nucleation by temperature variation in 100 nL microfluidic droplets.

Moreover, the fact that the crystal shape is rough hints at the shape of the critical nucleus. In the CNT, the shape of the critical nucleus is approximated by a sphere in order to simplify the excess term in the computation of the Gibbs free energy. An averaged interfacial energy, γ, is used in the computation as a consequence of the isotropic assumption on the critical nucleus shape. The crystal observed in Fig. 4(c) is in good agreement with this isotropic assumption, instead of presenting a faceted critical nucleus.

In the second set of experiments: first, we generated a high-supersaturated droplet of BPTI with the microinjector (Figs. 5(a)–5(d)) in order to stabilize it (with respect to nucleation) by volume confinement. Second, we used a sharp tip to induce a single nucleation event by touching the supersaturated metastable droplet of BPTI solution (Fig. 5(f)). We induced a structural transformation via mechanical contact at precisely determined points and times. This is in agreement with previous results obtained by Lenhoff group [28] in which as soon as a crystal touches the surface of a protein-rich

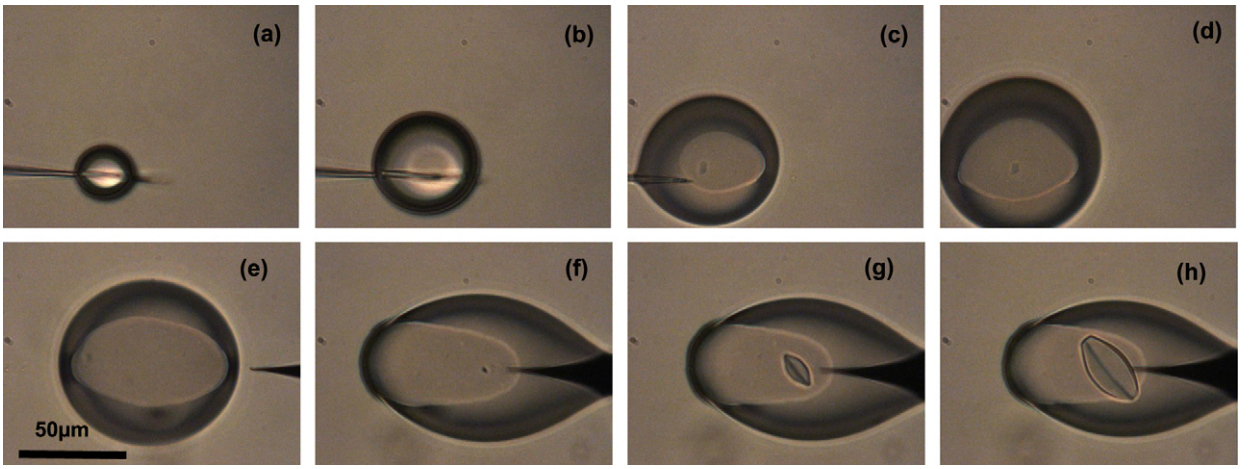

Fig. 5. ((a) to (d)) Generation of a BPTI droplet (20 mg/mL) in NaCl (1.6 M) in DMS oil and nucleation and growth of BPTI, (e) droplet size 85 µm (200 pL) at $t = 0$, (f) $t = 30$ min, (g) $t = 80$ min and (h) $t = 130$ min.

droplet, obtained by liquid–liquid phase separation, crystals instantaneously nucleate and grow. This seems to be a general rule: any disturbance triggers nucleation once a highly-supersaturated metastable state has been achieved.

4. Conclusions

In this communication, we present the use of small volumes, microdroplets, to control nucleation, conducting experiments with biological, organic and mineral molecules.

We use both microfluidic thermostatted devices allowing droplets to be formed in different aqueous and organic solvents and stored for several weeks without significant evaporation and a fluidic device that generates arrayed aqueous phase microdroplets in oil, with volumes ranging from nanoliter to femtoliter, without surfactant. We show that our microfluidic devices make it possible to study nucleation in both aqueous and organic solvents, and are applicable to organic molecules such as APIs, explosives or metal oxide nanoparticles.

For nucleation experiments conducted with the microfluidic set-ups, volume does not affect the nucleation process, which means they are representative of nucleation in infinite volumes, apart from a kinetic effect. However, nucleation experiments conducted in smaller volumes with our fluidic device are subject to an added thermodynamic effect, due to confinement, that stabilizes high-supersaturated solutions.

Lastly, we show, using a sharp tip (acting as a "magic wand") that a single nucleation event is launched as soon as the tip touches the supersaturated confined metastable solution. This spatial and temporal control is a major step forward in understanding the factors influencing the nucleation process.

Acknowledgements

We thank N. Ferté for protein characterization and fruitful discussions and Minh Phat La for technical assistance. We thank M. Sweetko for revising English.

References

[1] A.A. Chernov, Crystal growth science between the centuries, J. Mater. Sci., Mater. Electron. 12 (2001) 437–449.
[2] R. Grossier, S. Veesler, Reaching one single and stable critical cluster through finite sized systems, Cryst. Growth Des. 9 (2009) 1917–1922.
[3] R. Grossier, Z. Hammadi, R. Morin, A. Magnaldo, S. Veesler, Generating nanoliter to femtoliter microdroplets with ease, Appl. Phys. Lett. 98 (2011) 091916.
[4] E.W. Muller, T.T. Tsong, Field Ion Microscopy: Principles and Applications, American Elsevier Publishing Company, New York, 1969.
[5] Z. Hammadi, M. Gauch, R. Morin, Microelectron gun integrating a point-source cathode, J. Vac. Sci. Technol. B 17 (1999) 1390–1394.
[6] Z. Hammadi, J.P. Astier, R. Morin, S. Veesler, Protein crystallization induced by a localized voltage, Cryst. Growth Des. 8 (2007) 1476–1482.
[7] T. Detoisien, M. Forite, P. Taulelle, J. Teston, D. Colson, J.P. Klein, S. Veesler, A rapid method for screening crystallization conditions and phases of an active pharmaceutical ingredient, Org. Process Res. Dev. 13 (2009) 1338–1342.
[8] S. Lafont, S. Veesler, J.P. Astier, R. Boistelle, Solubility and prenucleation of aprotinin BPTI molecules in sodium chloride solution, J. Cryst. Growth 143 (1994) 249–255.
[9] R.C. Stevens, High-throughput protein crystallization, Curr. Opin. Struct. Biol. 10 (2000) 558–563.
[10] S.L. Anna, N. Bontoux, H.A. Stone, Formation of dispersions using "flow focusing" in microchannels, Appl. Phys. Lett. 82 (2003) 364–366.
[11] P. Laval, J.-B. Salmon, M. Joanicot, A microfluidic device for investigating crystal nucleation kinetics, J. Cryst. Growth 303 (2007) 622–628.
[12] L. Li, D. Mustafi, Q. Fu, V. Tereshko, D.L. Chen, J.D. Tice, R.F. Ismagilov, Nanoliter microfluidic hybrid method for simultaneous screening and optimization validated with crystallization of membrane proteins, Proc. Natl. Acad. Sci. 103 (2006) 19243–19248.

[13] J.-U. Shim, G. Cristobal, D.R. Link, T. Thorsen, S. Fraden, Using microfluidics to decouple nucleation and growth of protein, Cryst. Growth Des. 7 (2007) 2192–2194.
[14] T.M. Squires, S.R. Quake, Microfluidics: Fluid physics at the nanoliter scale, Rev. Mod. Phys. 77 (2005) 977.
[15] J. Leng, J.B. Salmon, Microfluidic crystallization, Lab Chip 9 (2009) 24–34.
[16] R.D. Dombrowski, J.D. Litster, N.J. Wagner, Y. He, Crystallization of alpha-lactose monohydrate in a drop-based microfluidic crystallizer, Chem. Eng. Sci. 62 (2007) 4802–4810.
[17] J.-B. Salmon, J. Leng, Microfluidics for kinetic inspection of phase diagrams, C. R., Chim. 12 (2009) 258–269.
[18] M. Ildefonso, N. Candoni, S. Veesler, A. Cheap, Easy microfluidic crystallization device ensuring universal solvent compatibility, Org. Process Res. Dev. 16 (2012) 556–560.
[19] M. Ildefonso, N. Candoni, S. Veesler, Using microfluidics for fast, accurate measurement of lysozyme nucleation kinetics, Cryst. Growth Des. 11 (2011) 1527–1530.
[20] E. Revalor, Z. Hammadi, J.P. Astier, R. Grossier, E. Garcia, C. Hoff, K. Furuta, T. Okutsu, R. Morin, S. Veesler, Usual and unusual crystallization from solution, J. Cryst. Growth 312 (2010) 939–946.
[21] M. Ildefonso, E. Revalor, P. Punniam, J.B. Salmon, N. Candoni, S. Veesler, Nucleation and polymorphism explored via an easy-to-use microfluidic tool, J. Cryst. Growth 342 (2012) 9–12.
[22] J.-M. Ha, J.H. Wolf, M.A. Hillmyer, M.D. Ward, Polymorph selectivity under nanoscopic confinement, J. Am. Chem. Soc. 126 (2004) 3382–3383.
[23] M. Beiner, G.T. Rengarajan, S. Pankaj, D. Enke, M. Steinhart, Manipulating the crystalline state of pharmaceuticals by nanoconfinement, Nano Lett. 7 (2007) 1381–1385.
[24] K. Kim, I.S. Lee, A. Centrone, T.A. Hatton, A.S. Myerson, Formation of nanosized organic molecular crystals on engineered surfaces, J. Am. Chem. Soc. 131 (2009) 18212–18213.
[25] C.J. Stephens, S.F. Ladden, F.C. Meldrum, H.K. Christenson, Amorphous calcium carbonate is stabilized in confinement, Adv. Funct. Mater. 20 (2010) 2108–2115.
[26] R. Grossier, A. Magnaldo, S. Veesler, Ultra-fast crystallization due to confinement, J. Cryst. Growth 312 (2010) 487–489.
[27] P. Laval, C. Giroux, J. Leng, J.-B. Salmon, Microfluidic screening of potassium nitrate polymorphism, J. Cryst. Growth 310 (2008) 3121–3124.
[28] D. Vivares, E.W. Kalera, A.M. Lenhoff, Quantitative imaging by confocal scanning fluorescence microscopy of protein crystallization via liquid–liquid phase separation, Acta Crystallogr. D 61 (2005) 819–825.